Supplementary Information for: Ammonium sensitivity of biological nitrogen fixation in anaerobic diazotrophs and coastal salt marsh sediments.

Romain Darnajoux[1], Linta Reji[1], Xin Rei Zhang[1,2], Katja E. Luxem[1], and Xinning Zhang[1, 2]

[1]Department of Geosciences, Princeton University, Princeton, 08544, NJ, USA

[2]High Meadows Environmental Institute, Princeton University, Princeton, 08544, NJ, USA

Corresponding author: RD and XZ

ORCID: RD: 0000-0002-4996-0067, XZ: 0000-0003-2763-1526, KEL: 0000-0001-7310-0668, LR: 0000-0002-1337-6782

SUPPLEMENTARY METHODS:

1) *Method S1: Contribution of BNF to new biomass production in pure culture of Desulfovibrio vulgaris var. Hildenborough (DvH)*

In order to estimate the contribution of BNF to new biomass production between two time points (Δt) during incubations (see Fig.1B), Eq. [1] expresses the new biomass created from measured BNF input ($dn_{cell,BNF}$) over total biomass increase ($dn_{cell,tot}$)

[eq 1] % BNF contribution = $[dn_{cell,BNF}/dn_{cell,tot}]_{\Delta t}$

Newly fixed N is approximated based on the amount of ethylene produced between timepoints using Eq. [2],

[eq 2] $dn_{N,BNF} = A*dppm_E$

and the total increase in biomass is approximated using the change in optical density as shown by Eq. [3]

[eq 3] $dn_{cell} = B*dOD_{600}$

In these equations, $dn_{N,BNF}$ is the quantity of N in mol, $dppm_E$ is the equivalent quantity of ethylene reduced in ppm v/v in headspace, dn_{cell} is the change in cell number, dOD_{600} is the change in turbidity at 600nm, and A and B are undetermined proportionality factors. The relative contribution of BNF to biomass production was derived from the control experiment without NH_4^+ addition, allowing us to estimate the parameter A using a rearrangement of Eq. [2]. The quantity of cells that originates from newly fixed N for any sample between two time points can now be expressed using [Eq.4].

[eq 4] $dn_{cell,BNF,\Delta t} = dn_{N,BNF,\Delta t}*[dn_{N,BNF}/dn_{cell,BNF}]_{ctrl}$

We substitute Eq. 4, 2 and 3 in 1, and after simplification of A and B, we can express the BNF contribution between each time point for data in Figure 1B using [Eq.5]

[eq 5] % BNF contribution = $[dppm_E/dOD_{600}]_{\Delta t,addition}$ /$[dppm_E/dOD_{600}]_{\Delta t,ctrl}$

2) Method S2: Calculation of residual NH_4^+ in media after biomass uptake

The residual ammonium concentration in medium after uptake for growth (presented in Supplementary Fig. S7) can be expressed as the initial quantity of NH_4^+ ($n_{NH4,media,0}$) minus the sum of the incremental quantities used by cells for growth over time ($dn_{NH4,cell,\Delta t}$):

[eq 6] $[NH_4^+]_t = n_{NH4,media} / V_{media} = (n_{NH4,media,0} - \sum dn_{NH4,cell,\Delta t}) / V_{media}$

Where V_{media} is the volume of media. For every Δt, the quantity of cells grown from media NH_4^+ ($dn_{cell,NH4,\Delta t}$) can be derived by rearranging Eq.[1] as the contribution of NH_4^+ to growth (estimated from BNF contribution to growth) multiplied by total cellular growth ($dn_{cell,tot,\Delta t}$):

[eq 7] $dn_{cell,NH4,\Delta t} = (1- \%\ BNF\ contribution_{,\Delta t}) * dn_{cell,tot,\Delta t}$

The amount of nitrogen necessary to produce 1 OD unit of biomass can be calibrated using the first growth plateau in sub-replete condition (*i.e.,* second lag-phase before the onset of BNF, see growth curve @ $[NH_4^+]$ =500 µM in main text Fig.1A), using Eq. [8]:

[eq 8] $dn_{NH4,cell,\Delta t} = dn_{cell,NH4,\Delta t} / [n_{NH4,media,0} / n_{cell,NH4,plateau}]_{sub\text{-}replete}$

allowing the calculation of ammonium uptake at each time Δt ($dn_{NH4,cell,\Delta t}$), and thus residual $[NH_4^+]$ using Eq.[6]. after simplification of B (from eq. [3]) and V_{media} (assuming constant media volume V_{media} over the experiment) using Eq. [9]:

[eq 9]

$[NH_4^+]_t = [NH_4^+]_{,media,0} - \sum (1- \%\ BNF\_contribution_{,\Delta t}) * dOD_{600,\Delta t} / ([NH_4^+]_{media,0} / OD_{600,plateau})_{sub\text{-}replete}$

SUPPLEMENTARY FIGURES

Figure S1

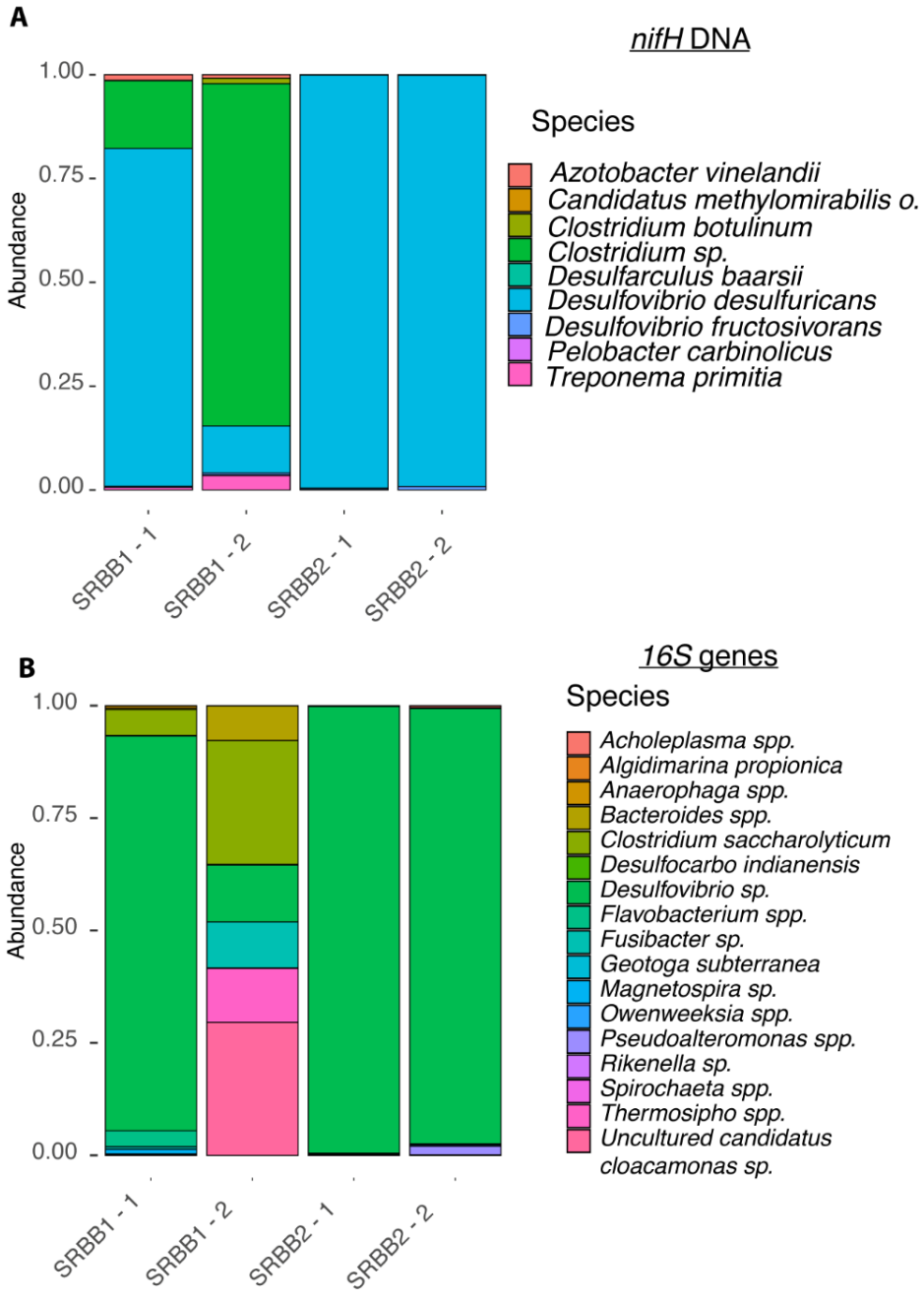

Figure S1: Microbial composition of SRBB1 and SRBB2 consortia based on *nifH* genes (A) and *16S* rRNA genes (B). Each consortium was cultivated in two replicates under the same conditions as in the experiment shown in Figure 2B. Nitrogen fixers in the consortia were dominated by *Desulfovibrio sp.*

FIGURE S2

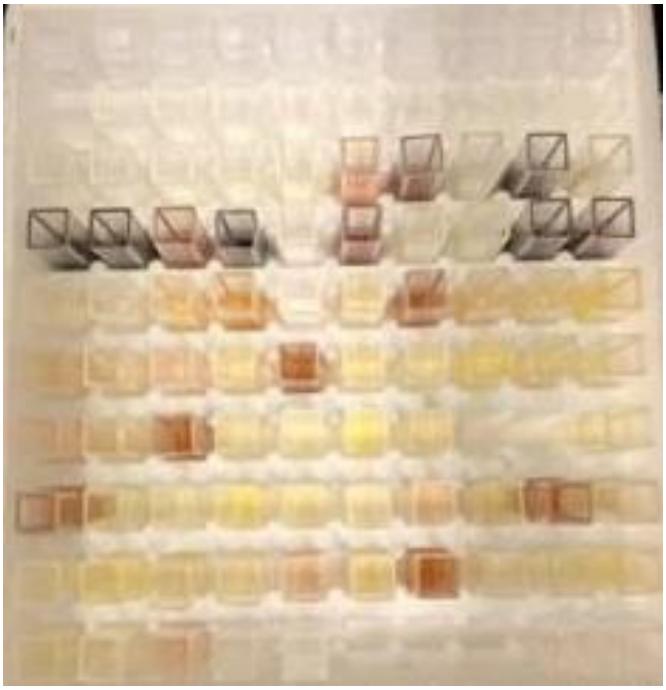

Figure S2: **Picture of filtered slurry samples after reaction with the o-phthalaldehyde (OPA) reagent**. The samples in the bottom of this picture are from early time points of the sediment ARA incubation, and show the white to yellow color expected in the OPA method. In the top of the picture, we see that the samples taken from 5 incubations after addition of ammonium (#4, #6, #7, #9, and #10) show abnormal dark orange to purple hues, even after 8-fold dilutions. No similar red-purple hues were observed with ^{15}N incubation samples.

FIGURE S3

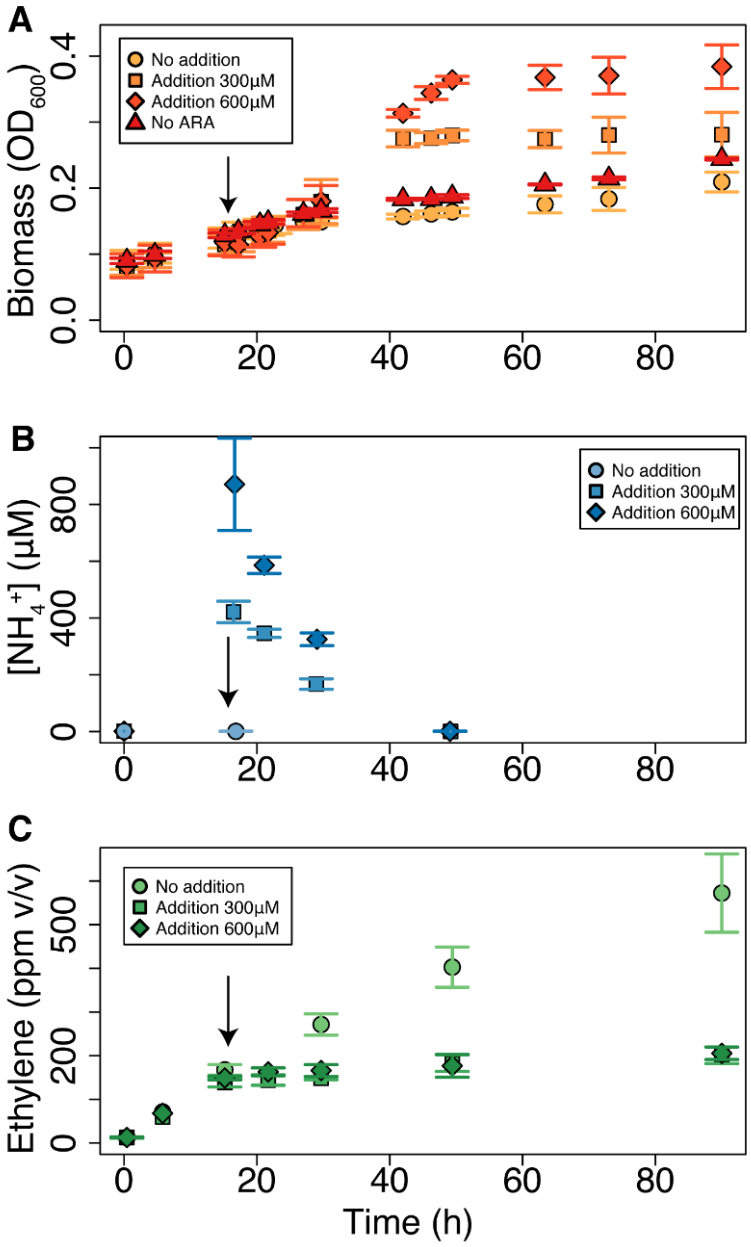

Figure S3: **Effect of ammonium concentration on the acetylene reduction activity of *Desulfovibrio vulgaris* var. Hildenbourough (DvH)**. The change in biomass (A), ammonium concentration (B), and headspace ethylene was monitored during incubation (C) with (square and diamond) and without (circle) added NH_4^+. In panel A, comparison of growth rate and yield with and without addition of ~2.5%v/v acetylene (circle vs. triangle) illustrates limited inhibition (30-40% decrease in growth rate) of acetylene on DvH. Error bars are standard error of three technical replicates.

FIGURE S4

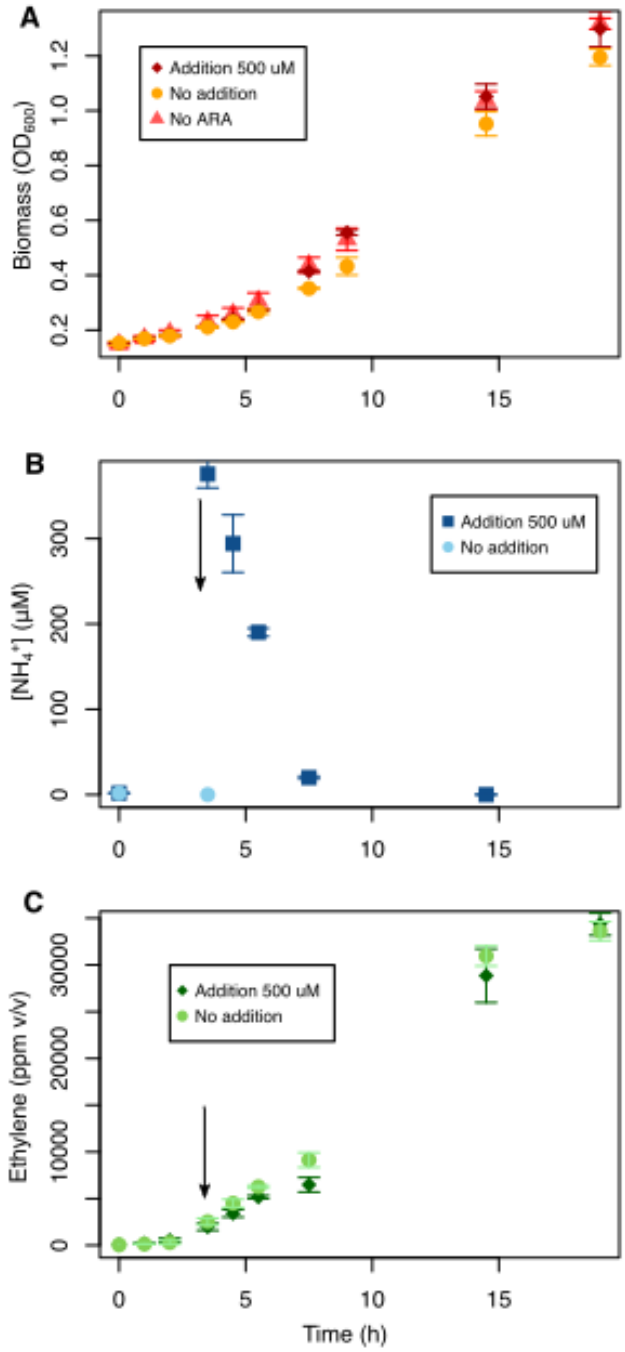

Figure S4: **Effect of ammonium concentration on the acetylene reduction activity of *Clostridium pasteurianum* strain W3 (Cp)**. The change in biomass (A), ammonium concentration (B), and headspace ethylene was monitored during incubation (C) with (square and diamond) and without (circle) added NH_4^+. In panel A, comparison of growth rate and yield with and without addition of ~2.5%v/v acetylene (circle vs. triangle) illustrates limited inhibition (~5% decrease in growth rate) of acetylene on *Cp*. Error bars are standard error of three technical replicates.

FIGURE S5

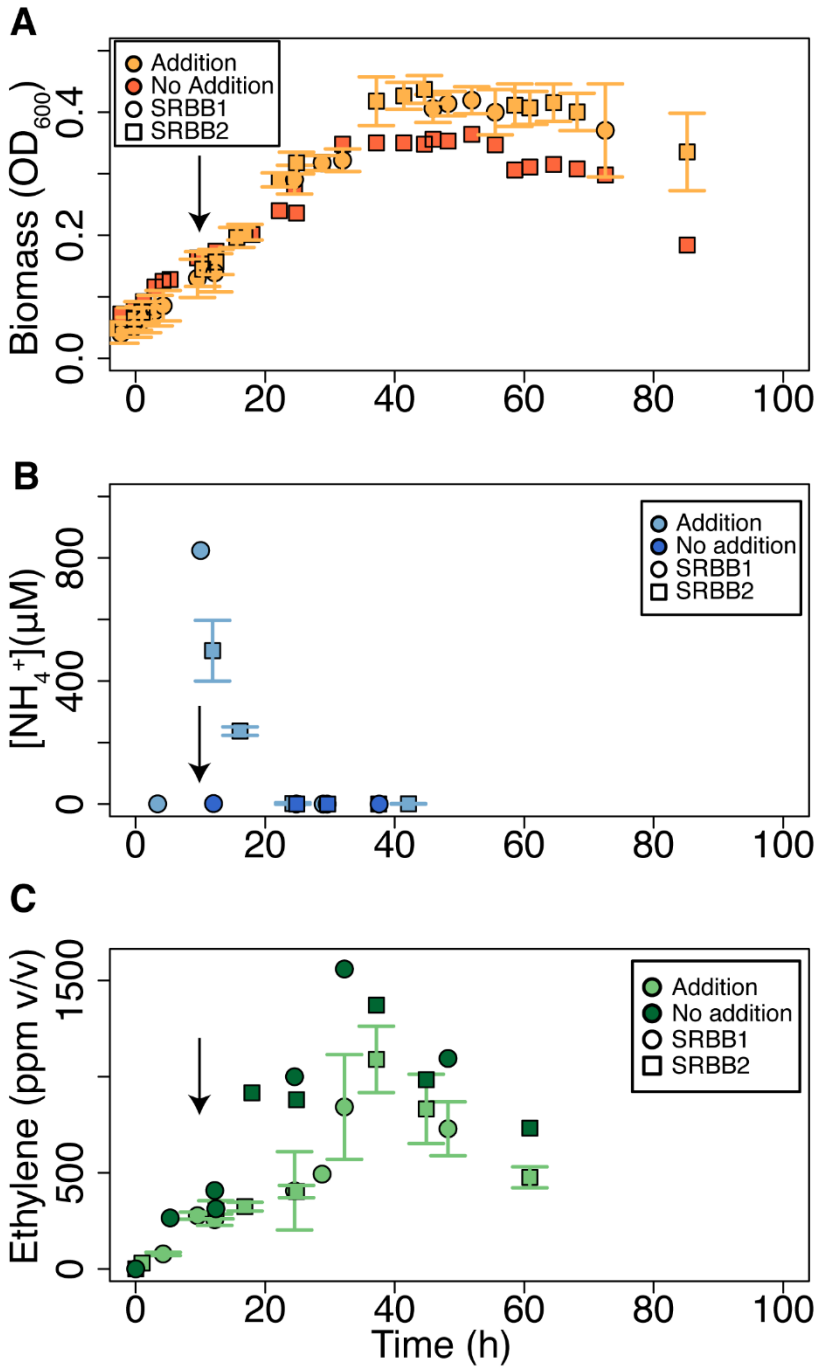

Figure S5: **Effect of ammonium concentration on acetylene reduction activity in two enrichment cultures from Barnegat Bay salt marshes sediments** (SRBB1 and SRBB2, see main text M&M). The evolution of biomass (A), ammonium concentration (B), and headspace ethylene (C) during ARA experiments with (dark) and without (light) added NH_4^+ are shown. Error bars show the standard error of three technical replicates.

Figure S6

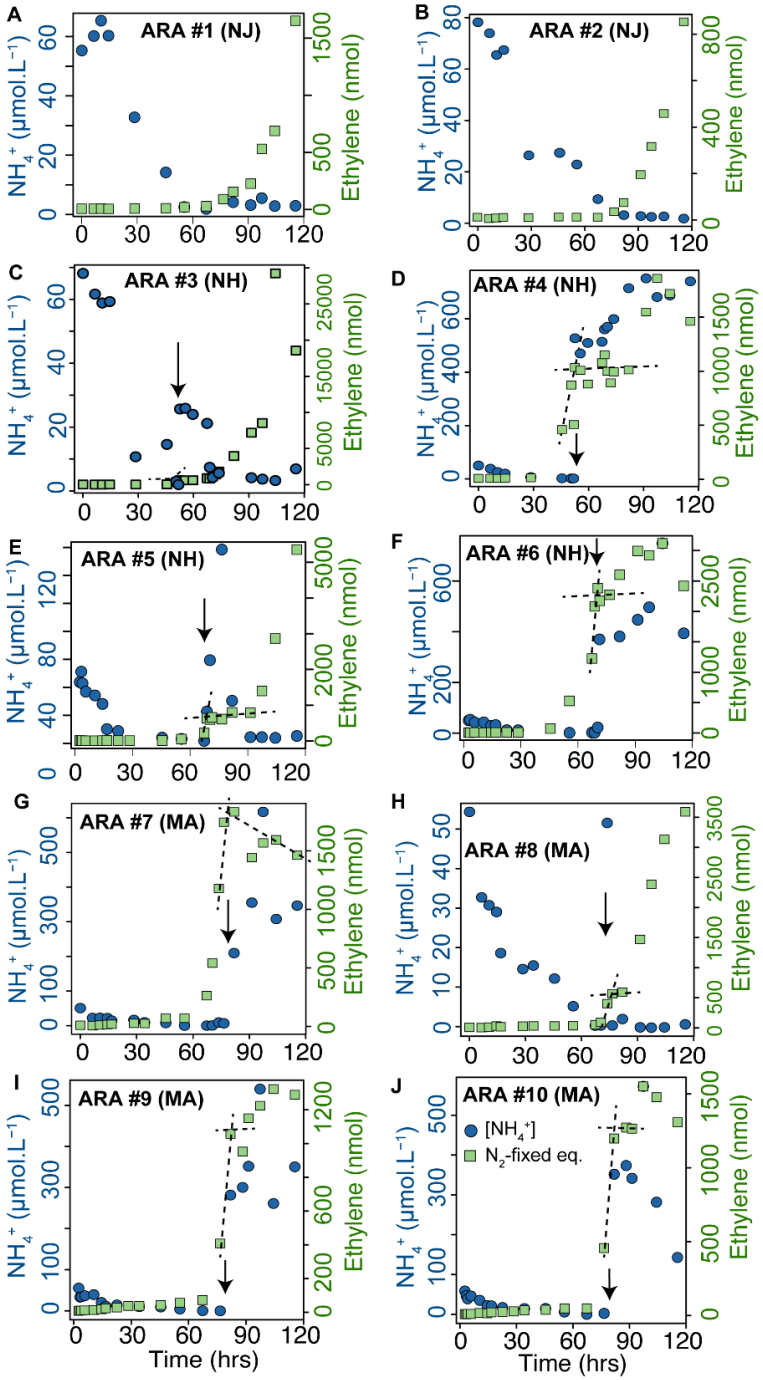

Figure S6: **Effect of ammonium concentration on the acetylene reduction activity of salt-marsh sediments.** Dissolved [NH_4^+] (blue circles) and Biological Nitrogen Fixation (BNF) activity evaluated using Acetylene Reduction Assay (green squares) over time in salt marsh sediments from Barnegat Bay, New Jersey (NJ, A and B), Great Bay, New Hampshire (NH, C to F), and Sippewissett, Massachusetts (MA, G to J) in slurry incubations with no NH_4^+ amendment (A and B) and with NH_4^+ additions (C to J). Additions are indicated with arrows. Dashed lines illustrate interpolation of the BNF rate before and after NH_4^+ addition to estimate the time to BNF inhibition (T_R).

Figure S7

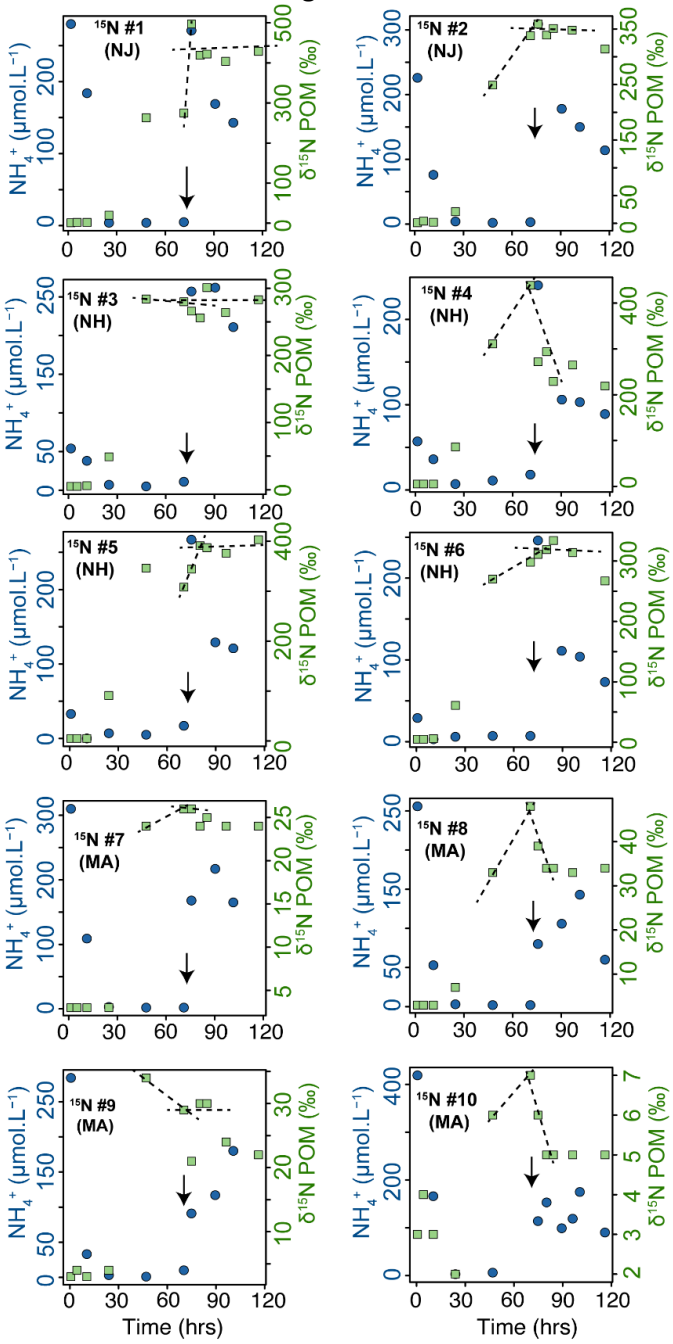

Figure S7: **Effect of ammonium concentration on ^{15}N- Biological Nitrogen Fixation (BNF) activity in salt-marsh sediments.** Dissolved [NH_4^+] (blue circles) and BNF activity evaluated using ^{15}N tracer experiment (green squares) over time in salt marsh sediment from Barnegat Bay, New Jersey (NJ, A and B), Great Bay, New Hampshire (NH, C to F), and Sippewissett, Massachussett (MA, G to J) in slurry incubations with no NH_4^+ amendment (A and B) and with NH_4^+ additions (C to J). Additions are indicated with arrows. All sediment samples except #3 to #6 received addition of ammonium before starting the experiments. Dashed lines illustrate the interpolation of the BNF rate before and after NH_4^+ addition that was used to estimate the time to BNF inhibition (T_R).

Figure S8

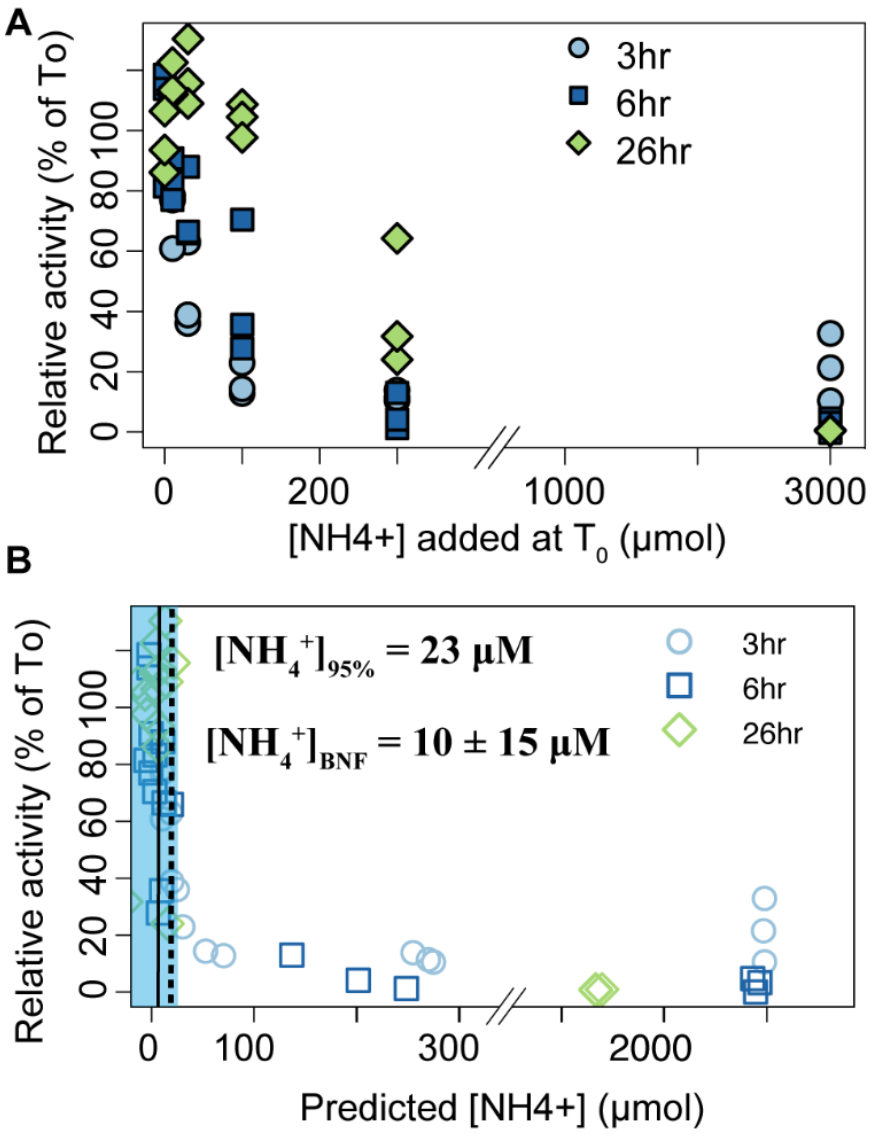

Figure S8. Effect of timing and initial concentration on residual ammonium media concentration and Biological Nitrogen Fixation (BNF) activity. Relative BNF activity measured using Acetylene Reduction Assay at 3h, 6h and 26h after additions of NH_4^+ (to reach concentration of 10, 30, 100, 300, and 3,000 µM, see main text Figure 1B) compared to BNF activity before NH_4^+ addition for *Desulfovibrio vulgaris* var. Hildenborough initially grown under N_2-fixing conditions as a function of initially added concentration (A) and calculated residual [NH_4^+] in the media at the time of sampling (B), as calculated according to Supplementary Methods S2. Symbols represent individual samples from a single experiment. Blue boxes indicate the range of ammonium values showing detectable BNF (>20%), the black lines indicate the average values, and dotted lines the 95-percentile (*i.e.*, threshold value).

FIGURE S9

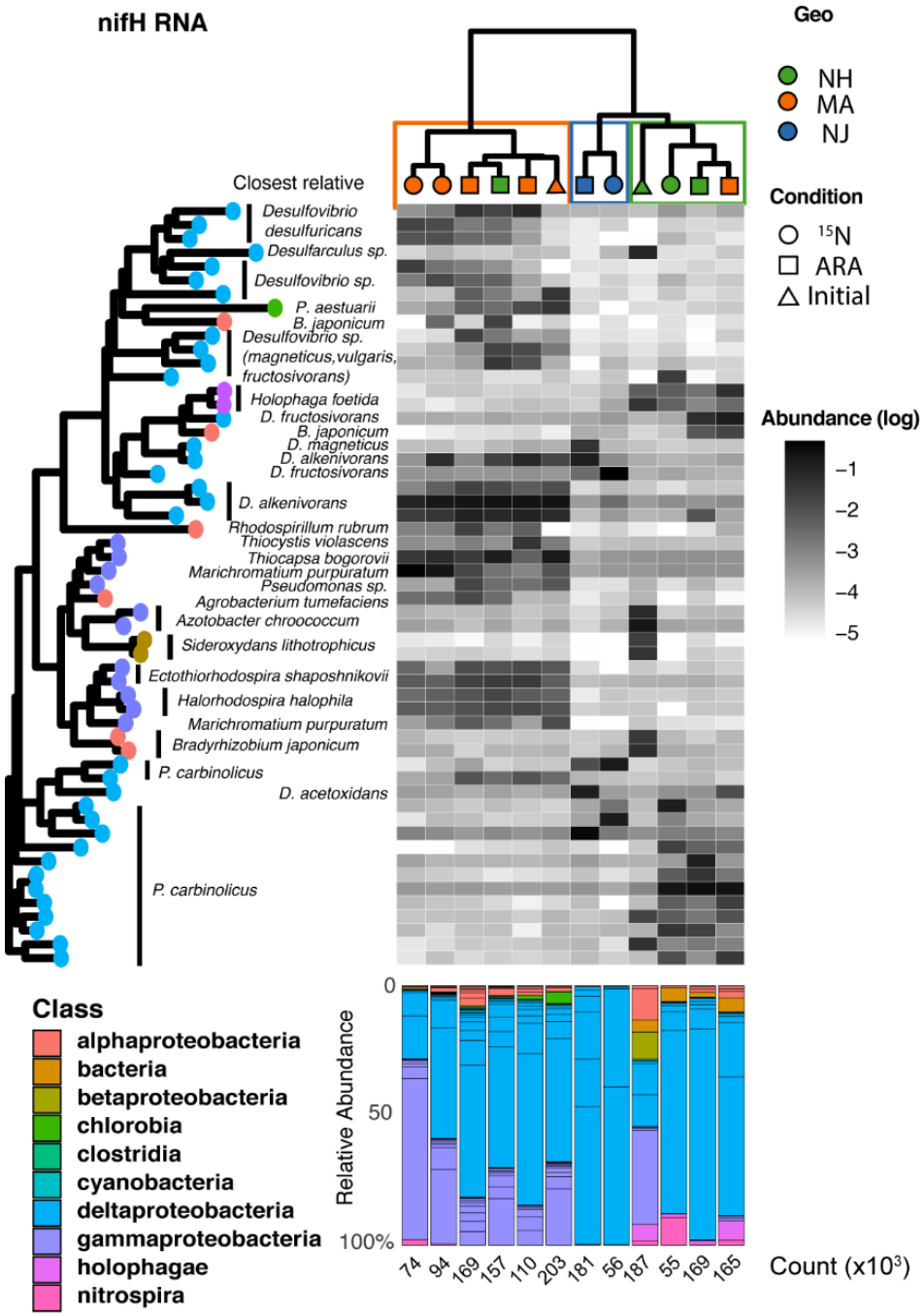

Figure S9: Microbial composition of diazotroph community in salt marsh sediment incubations. Heatmap of *nifH* RNA relative abundance (log-scale) at the end of incubation with class-level information for the 200 first OTUs (bottom bar plot, > 85 % total abundance) and detailed phylogeny and closest relatives for the most abundant sequences (left panel, OTUs with relative abundance >0.2% & total count >1000, n=55). Hierarchical clustering of individual sediment samples based on *nifH* composition (top left of panel) shows the relationship between sample *nifH* RNA composition, incubation condition (ARA vs. ^{15}N), and geographical origin of the sediments.

FIGURE S10

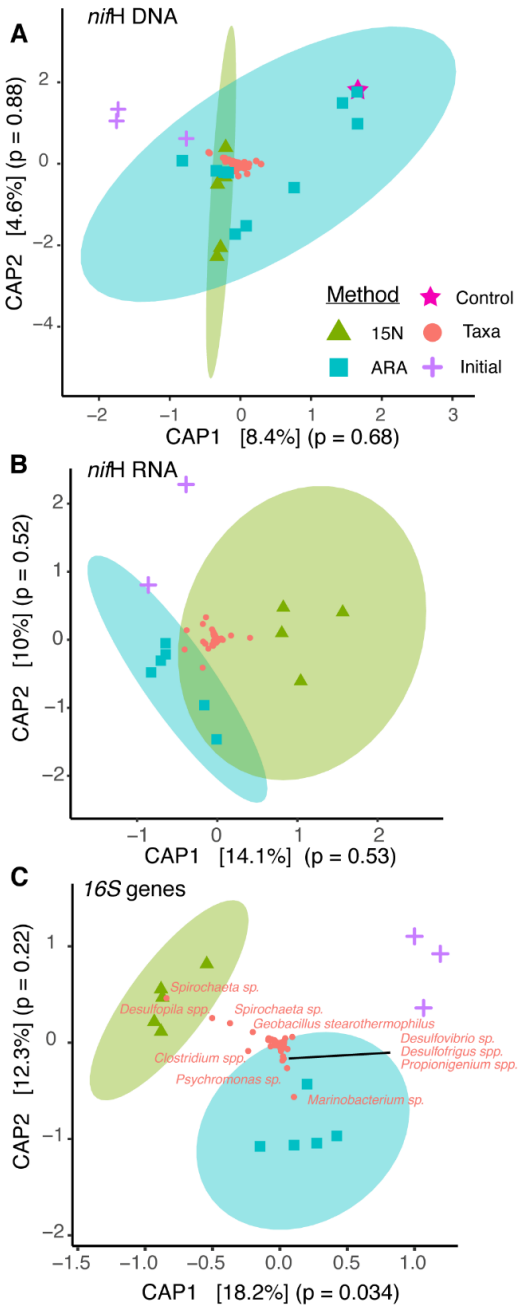

Figure S10: **Effect of acetylene (2.5%v/v) on the microbiomes of sediments after five day in slurry incubation.** Discrimination analysis using Canonical Analysis of Principal coordinates (using Bray-Curtis distance) on (A) *nifH* genes, (B) *nifH* transcript, et (C) *16S* rRNA genes. Axes show the percent of variance explained and the statistical significance for each explanatory axis as estimated using permutation Anova. Blue and green disc highlight the 95% confidence ellipses. Results were unchanged when we control for the origin of the sediment (NJ, NH, and MA), or when we remove the initial and control data. In panel C, species that are over-represented in one group are listed in red.

FIGURE S11

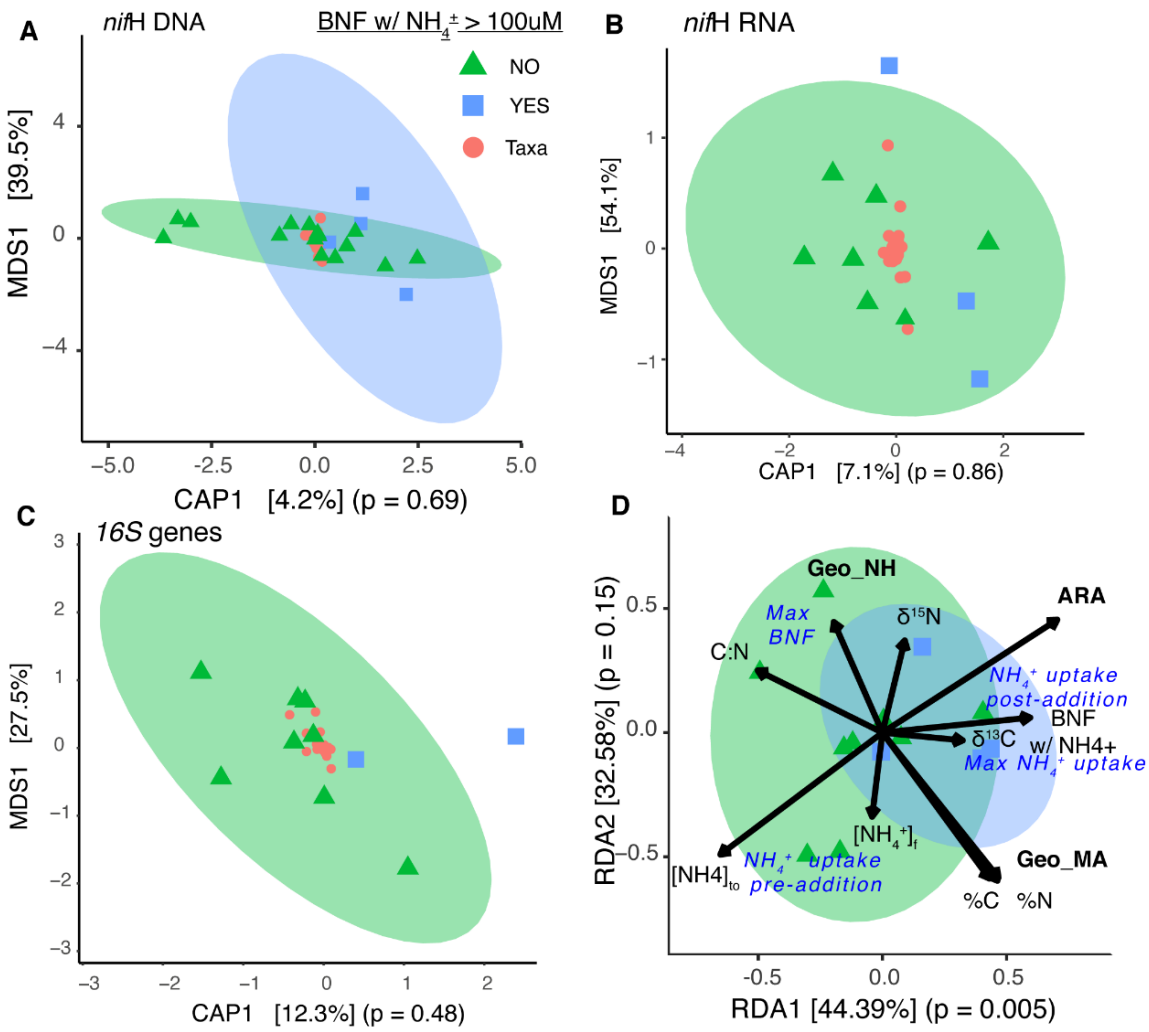

Figure S11: Discrimination analysis of samples showing increase ethylene production at high ammonium. Canonical Analysis of Principal Coordinates on Bray-Curtis distance of microbial communities for (A) *nifH* genes (n=4), (B) *nifH* transcript (n=3) and (C) *16S* genes (n=2), and Redundancy Analysis on normalized biogeochemical data (D, n=4) on samples (total 4/20) showing increased headspace ethylene with post addition $[NH_4^+]$ > 100µM. Axes show the percent of variance explained and the statistical significance for each explanatory axis as estimated using permutation Anova. Results were unchanged when controlled for the origin of the sediment (NJ, NH, and MA) or the method used to assess BNF activity (^{15}N tracer vs. Acetylene Reduction Assay). Blue and green disc represent the 95% confidence ellipses for each group. In panel D, variables in bold are significantly influencing the model.

FIGURE S12

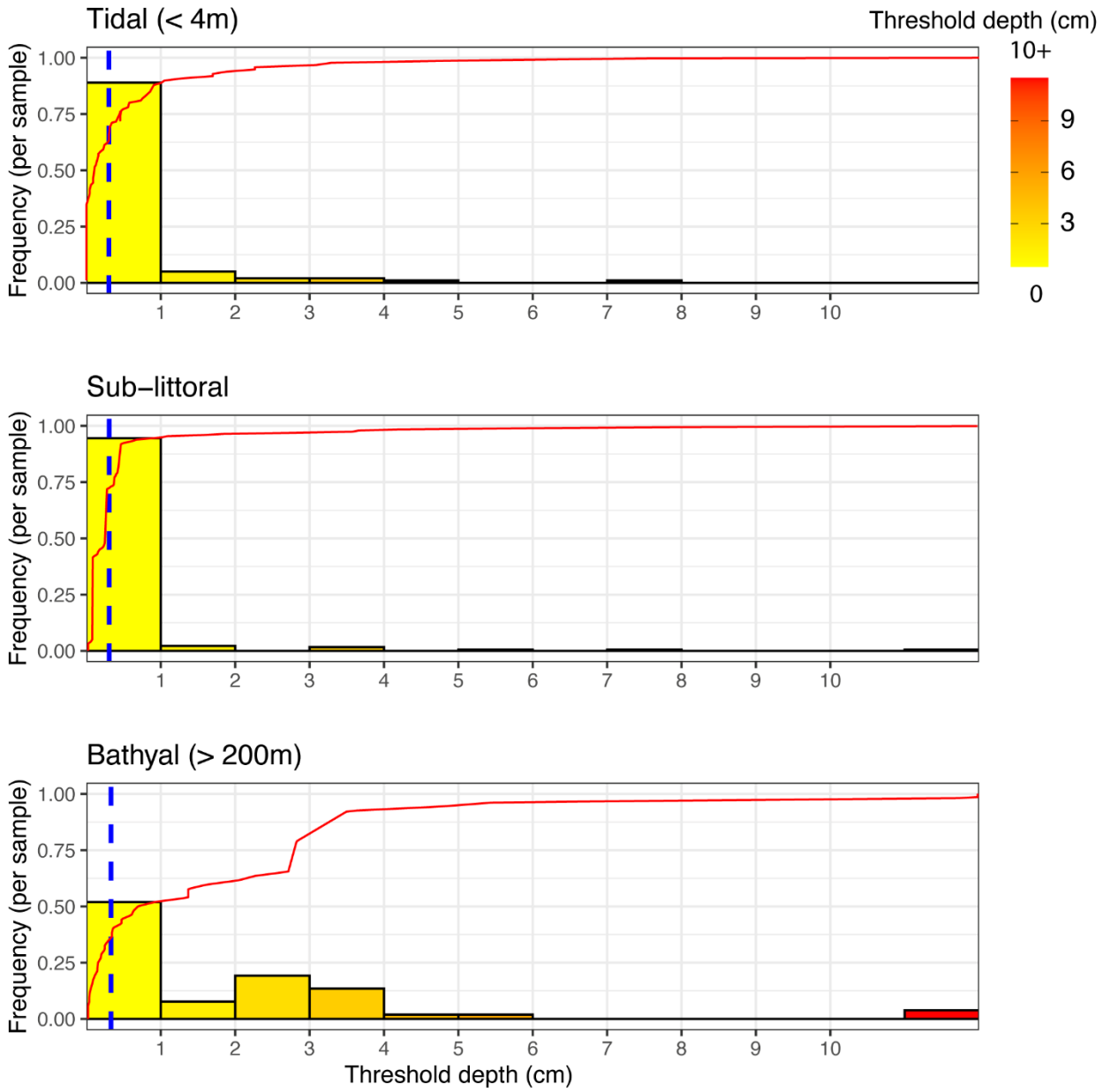

Figure S12: Frequency distribution of threshold depth per benthic zones. Threshold depth (*i.e.*, depth at which $[NH_4^+]_{threshold}$ was reached) were derived from literature review of 26 study (151 sites, 334 replicates, see Table S1). Benthic zones were separate according to reported water depth as tidal (< 4 m, n= 64), sub-littoral (between 4 and 200 m, n=47), and bathyal (> 200 m, n=40) The red lines represent cumulative frequencies, and the dashed vertical line represent the median value.

SUPPLEMENTARY DISCUSSION

OBSERVATIONS:

We identified four instances that could be interpreted to suggest that nitrogenase activity is not sensitive to high ammonium concentrations, contrary to the main conclusion of our work. Here, in this Supplementary Discussion, we describe these observations and why we have concluded that they are most likely misleading artefacts rather than a true biological phenomenon.

Several filtered supernatant aliquots representing several timepoints sampled from five sediment incubations assessed by ARA (#4, #6, #7, #9, #10, Fig. S5) after NH_4^+ addition exhibited irregular coloration (red-black instead of yellow) during the OPA procedure, even after 8-fold dilution (Fig. S2). In four of these five samples (two each from the NH and MA salt marshes), an increase in headspace ethylene was observed ~ 10h after an initial plateau following NH_4^+ addition, even though measured [NH_4^+] remained > 100 μM at this time (Fig. S5 #4, #6, #9&#10). These observations of increased headspace ethylene levels were limited to a few timepoints, showed a step-like behavior in two of the four occurrences, and stopped before the end of the experiment (see Fig. S5). For four of the eight ARA sediment samples (two each from NH and MA salt marshes) spiked with NH_4^+, BNF rates also resumed within ~ 10h after addition, but ambient NH_4^+ was drawn down to near background levels ([NH_4^+] < 10 μM, Main article Fig. 2C, Fig. S5) within this timeframe, likely due to assimilatory or dissimilatory biological activities. Together, these observations suggest that the "measured" ammonium concentration calculated based on sample absorbance during the OPA assay might be incorrect in these samples. Indeed, two of these four samples even showed an increase in NH_4^+ concentration in the absence of further exogenous ammonium addition. Importantly, none of the 10 sediment incubations assayed using the ^{15}N tracer method, which directly reflect BNF activity, showed any evidence of a resumption of BNF activity after NH_4^+ amendment, and post addition NH_4^+ concentration never decreased below 50 μM (Fig. S6).

DISCRIMINATION ANALYSES:

To confirm that the microbiome in samples with abnormally colored OPA samples (5 out of 20 experiments, Fig. S5), where we observed increases in headspace ethylene concentrations coincident with the appearance of high

ammonium (>100 uM), is similar to the other samples, we performed a discriminant analyses on the *nifH* microbiome data (CAP on Bray-Curtis dissimilarities, Fig. S10) from our ARA and ^{15}N incubations. We could not distinguish these four samples from others exhibiting the classical response of BNF inhibition by ammonium based on their microbial composition (*nifH* and *16S* genes), even when controlling for the geographic origin of sediments as the covariate (Fig. S10 panel A-C). This implies that there is no single organism or assemblage of diazotrophs, as assessed by *nifH* or 16S at the end of incubation, that can easily explain our anomalous observations of BNF. We also found good correlation between the presence of ethylene production at high NH_4^+ concentration and the maximum NH_4^+ depletion rate using redundancy analysis on the biogeochemical data (Fig. S10 panel D), but the high confoundedness between variables prevents a more definitive interpretation.

SUMMARY AND CONCLUSION:

In four instances from two sites (MA and NH), we found results that could be interpreted as evidence that nitrogenase activity is not sensitive to high ammonium concentrations (Fig. S5 #4, #6, #9 & #10). This could suggest changes in ammonium uptake and regulatory mechanisms of BNF in a suite of specialized diazotrophs. There are, however, several arguments against such a conclusion; i) in all of these ARA samples, BNF activity initially stopped for 7-20 h directly after ammonium addition, indicating the active diazotrophs were sensitive to ammonium, ii) ethylene production resumed for less than 30h with lower activity, step-wise increase, and all samples stopped producing ethylene by the end of the incubation, iii) no OTUs based on *16S* and *nifH* analyses could be specifically linked to these four samples, and iv) we did not found evidence of similar phenomena in any of our ^{15}N tracer incubations. Possible explanations for anomalous findings in the 4 samples range from artifacts of long incubation (5 days), where high biomass increase could foster the development of microniches of depleted ammonium, methodological flaws (OPA measurement of ammonium, headspace sampling, agitation), and human error. After careful consideration, these specific data points were annotated where included in the main article (Figure 3B) and removed from further analyses.